



CrossMark
click for updates

Cite this: *RSC Adv.*, 2014, 4, 54187

Promotion of low-temperature oxidation of CO over Pd supported on titania-coated ceria†

Atsushi Satsuma,^{*ab} Masatoshi Yanagihara,^a Kaoru Osaki,^a Yurina Saeki,^a Heng Liu,^a Yuta Yamamoto,^c Shigeo Arai^c and Junya Ohyama^{ab}

The design of a metal oxide support for Pd was investigated to promote the oxidation of CO at lower temperatures. Through a screening study using pure metal oxides, Pd/CeO₂ showed the highest activity above 100 °C, while homemade TiO₂ was more effective below 100 °C as a support for Pd. Applying the advantages of CeO₂ and TiO₂, we proposed a TiO₂-CeO₂ support having a monolayer amount of surface TiO₂ supported on CeO₂. The Pd/TiO₂-CeO₂ catalyst showed higher activity than both Pd/TiO₂ and Pd/CeO₂, which was not achieved by using the CeO₂-TiO₂ mixed-oxide. The light-off temperature over Pd/TiO₂-CeO₂ was 100 °C lower than Pd/Al₂O₃. The effect of surface TiO₂ was attributed to the promotion of the reduction-oxidation cycle of supported Pd.

Received 10th September 2014
Accepted 17th October 2014

DOI: 10.1039/c4ra10167g

www.rsc.org/advances

1. Introduction

In order to reduce carbon dioxide (CO₂) emissions from automobiles, better fuel economy systems, such as hybrid and start-stop systems, are becoming popular. The exhaust gas temperature of these systems is lower than ever because of better energy efficiency. Hence, the enhancement of low-temperature activity is strongly required for automobile catalysts, especially for combustion of CO and unburned hydrocarbons as the main components in low-temperature exhaust fumes.

Among platinum group metals (Pt, Pd, and Rh) as active elements in a three-way catalyst, a supported Pd catalyst is one of the essential components playing important role in the combustion of CO and unburned hydrocarbons. For the promotion of low-temperature activity of a supported Pd catalyst, we can find various strategies for catalyst design in the literature. Generally, the catalytic activity is correlated to the dispersion of supported Pd. For example, Baylet *et al.* reported that both higher surface area of supports and stability of Pd particles are required to achieve higher Pd dispersion on hexaaluminate.¹ The higher dispersion of Pd can be obtained by metal-support interaction under cycles between oxidative and reductive atmospheres encountered in an exhaust gas. Nishihata *et al.* developed so called “intelligent catalyst” based on Pd-

loaded perovskite on which supported Pd retained its high metal dispersion by reversible incorporation of Pdⁿ⁺ ions under oxidative atmosphere and formation of Pd⁰ particles under reductive atmosphere.² The similar effect on the retention of metal dispersion is observed when CeO₂ and CeO₂-based supports are used as supports by forming solid solutions or the formation of metal-O-Ce bonds.^{3,4}

The catalytic activity of supported Pd is sometimes more affected by the oxidation state of Pd. For example, we have reported very unique dependence of the oxidation activity of Pd/CeO₂ on surface area of the CeO₂ support, *i.e.*, the lower surface area of CeO₂ was more preferable for the propene oxidation depending on the reaction and pre-treatment conditions.⁵ In this case, the propane oxidation at 200 °C proceeds preferably on metallic Pd species which is more stable in larger Pd particles on CeO₂ having low surface area. The metallic Pd species plays an important role on the oxidation reaction at lower temperatures, such as CO oxidation.^{6,7} On the other hand, oxidized Pd species shows higher activity for the methane oxidation,⁸⁻¹² which is rationalized by the role of dispersed Pd oxide species as an oxygen provider.¹³⁻¹⁵ The oxidation state of supported Pd is strongly affected by the acid-base property of supports.^{3,10} It is also known that incorporated Pd species in metal oxide matrix shows activity for the oxidation reactions. Hedge and co-workers proposed “noble metal ionic catalysts” in the formulae of Ce_{1-x}Pd_xO_{2-δ} and Ce_{1-x-y}Ti_yPd_xO_{2-δ} ($x = 0.01-0.02$, $\delta \approx x$, $y = 0.15-0.25$) and Ti_{1-x}Pd_xO_{2-x} ($x = 0.01-0.03$), which showed very high CO oxidation activity below 100 °C.¹⁶⁻²¹ Kurnatowska and co-workers also reported that nanocrystalline Ce_{1-x}Pd_xO_{2-y} exhibited a good performance on the low-temperature CO oxidation.²² In these catalysts, the low-temperature activity is assigned to the formation of Pd-O-Ce bond as a redox site and activation of lattice oxygen. Actually,

^aGraduate School of Engineering, Nagoya University, Nagoya 464-8603, Japan. E-mail: satsuma@apchem.nagoya-u.ac.jp; Fax: +81-52-789-3193; Tel: +81-52-789-4608

^bUnit of Elements Strategy Initiative for Catalysts & Batteries, Kyoto University, Kyoto 615-8530, Japan

^cEcotopia Science Institute, Nagoya University, Nagoya, 464-8603, Japan

† Electronic supplementary information (ESI) available: XRD patterns of Pd supported catalysts, TEM/EDS micrographs of TiO₂-CeO₂ support, and the estimation of oxygen storage-release rate from TG-DTA. See DOI: 10.1039/c4ra10167g

Colussi *et al.* clearly demonstrated by means of HRTEM and DFT calculations that Pd–O sites in Pd–Ce surface enhanced the catalytic activity for methane combustion.²³

As for the role of supports, oxygen storage and release capacity (abbreviated as OSC, hereafter) strongly controls the catalytic activity especially at lower temperatures. Liu *et al.* demonstrated an effective contribution of iron oxide support to low-temperature CO oxidation.²⁴ They reported that CO oxidation over Pt/FeO_x and Pd/FeO_x proceeds over two adjacent but different active sites (Pt, Pd for CO and FeO_x for oxygen) with low apparent activation energies (30–34 kJ mol⁻¹). Ikeue *et al.*, reported that the use of partially Fe-substituted 10Al₂O₃·2B₂O₃ as a support of Pd gave an effective catalyst for the catalytic NO conversion in a fuel rich region because of improved oxygen storage capacity.²⁵ In the case of CeO₂-based supports, it is well known that partial incorporation of Zr and other elements in CeO₂ lattice significantly improves OSC.^{26–31} Several papers demonstrated suitable designs of CeO₂-based metal oxide supports for promotion of CO oxidation activity using CeO₂,^{32–34} CeO₂/Co₃O₄,^{35–37} and CeO₂-TiO₂.^{38–44} There are two major effects of CeO₂-based supports on the low temperature oxidation: one is the promotion of redox cycles of Pd particles, and another is supply of lattice oxygen.⁷ As for the latter effect, the strong adsorption of CO on Pd surface strongly suppresses O₂ adsorption and activation on Pd particles in Pd/Al₂O₃ at lower temperatures, while CeO₂-based supports played a role of oxygen supply from lattice even when the Pd surface is fully covered by strongly adsorbed CO.⁷

On the basis of above mentioned activity-controlling factors for supported Pd catalysts, the present study aimed a design of novel supported Pd catalysts for low-temperature oxidation of CO. We focused TiO₂ having a limited promotion effect only at lower temperatures. Although mixed oxide of CeO₂-TiO₂ has been already proposed,^{38–44} this study proposed hierarchical configuration of TiO₂ and CeO₂ for the better CO oxidation activity at lower temperatures.

2. Experimental section

Supported Pd catalysts with Pd content of 1 wt% were prepared by a conventional impregnation method using an aqueous palladium nitrate, followed by dryness and calcination in air at 500 °C for 3 h. CeO₂ (JRC-CEO-3), TiO₂(B) (JRC-TIO-8), ZrO₂ (JRC-ZRO-1) were supplied from the committee of reference catalyst, Catalysis society of Japan. SiO₂ (Fuji Silysia, Q10) and Fe₂O₃ (Kishida Chemical, 98%) were purchased. Al₂O₃ was obtained by calcination of boehmite at 900 °C in air for 3 h. TiO₂(A) was prepared by hydrolysis of Ti(OC₃H₇)₄ (Kishida Chemical, 99%) by an aqueous solution of ammonia followed by dryness and calcination in air at 500 °C for 3 h. CeO₂-TiO₂ (Ce/Ti = 0.2) and TiO₂-ZrO₂ (Ti/Zr = 5/5) were prepared by co-precipitation^{37–45} using TiCl₄ (Kishida Chemical, 24%), Ce(NO₃)₄ (Kishida Chemical, 98%) and ZrO(NO₃)₂·2H₂O (Kishida Chemical, 99%) as precursors. The mixed aqueous solutions were neutralized with an aqueous solution of ammonia (Kishida Chemical, 28%), and the obtained precipitates were dried and then calcined in air at 500 °C for

3 h. TiO₂-CeO₂ supports were prepared by a precipitation method as follows. CeO₂ powder and distilled water were put in a beaker. After the temperature regulation of the beaker in a water bath, a prescribed amount of Ti source (TiCl₄ or Ti(OC₃H₇)₄) was added to the solution and stirred for 30 min. Then an aqueous solution of ammonia was added to adjust pH of the solution around pH = 8–9. The precipitates were filtrated and washed with distilled water, and then dried and calcined at 500 °C for 3 h in air. The detailed preparation conditions are described in the Section 3.2.

The catalytic activity was evaluated by CO oxidation using a conventional fixed-bed flow reactor at atmospheric pressure with a 10 mg of catalyst at a total flow rate of 100 N cm³ min⁻¹ which corresponds to GHSV = 480 000 h⁻¹.⁷ A catalyst was at first reduced in a flow of 3% H₂/He at 400 °C for 10 min, and the catalytic run was carried out under a flow of 0.45% CO/10% O₂/N₂. The effluent gas was analyzed by nondispersive infrared (NDIR) CO/CO₂ analyzer (Horiba VIA510).

Temperature programmed reduction by CO (CO-TPR) was carried out using a conventional fixed-bed flow reactor as follows. The sample was oxidized in a flow of 20% O₂/N₂ (100 N cm³ min⁻¹) at 400 °C for 30 min. After cooling the sample in a flow of pure N₂ to room temperature, the CO-TPR measurement was carried out in a flow of 0.4% CO/N₂ at a rate of 5 °C min⁻¹ up to 400 °C. The effluent gas was analyzed by nondispersive infrared (NDIR) CO/CO₂ analyzer (Horiba VIA510).

The dispersion of Pd was estimated by the CO-pulse adsorption method.^{46–48} A catalyst was at first treated in a flow of O₂ at 400 °C for 15 min followed by purge with He for 15 min, and then reduced in a flow of H₂ at 400 °C for 15 min followed by purge with He for 15 min. Then the catalyst was cooled in a flow of He, and a series of CO pulses were injected with an interval of 2 to 3 min until the amount of slipped CO pulses reaches a steady state value. In order to avoid oxidation of CO to CO₂ followed by adsorption on CeO₂ as carbonate, the sample cell was soaked in a dry ice/ethanol bath and the adsorption of CO was carried out at *ca.* -70 °C. The BET specific surface area was measured by N₂ adsorption at liquid N₂ temperature by using a conventional flow-type adsorption apparatus.

The oxygen storage-release property was evaluated by weight deviation under the following O₂-H₂ periodic operation at 300 °C using TG-DTA (Shimadzu DTG-60H). In order to suppress the reduction-oxidation of supported Pd, the oxidation step was carried out under low oxygen concentration (3%). After pretreatment in a flow of 3% O₂/N₂ at 500 °C for 30 min, the oxidized sample was cooled down to 300 °C in 3% O₂/N₂. After purging with pure N₂ for 30 s, a flow gas was switched to 3% H₂/N₂ until the catalyst weight loss reaches to a steady state. Then the purging in pure N₂, oxidation in 3% O₂/N₂ until the catalyst weight recovered, the purging in pure N₂, and the reduction in 3% H₂/N₂ were repeated for several times at 300 °C.

Pd K-edge XANES spectra were measured on BL28B2 of SPring-8 (Hyogo, Japan) operated at 8 GeV. The analyses of X-ray Absorption Near Edge Structure (XANES) were performed using the REX version 2.5 program (RIGAKU).

3. Results and discussion

3.1. Screening study

At first, a screening study of the effect of support materials on the oxidation of CO was carried out as summarized in Table 1. The temperatures at which the CO conversion reached to 20% and 80% (T_{20} and T_{80}) were used as indexes of light-off and nearly complete oxidation, respectively. It should be noted that the results were reproducible as far as the activity tests were carried out below 500 °C. The values of T_{20} for Pd catalysts supported on TiO_2 , CeO_2 , and CeO_2 -based mixed oxides were below 100 °C, while those were higher than 130 °C when Al_2O_3 , SiO_2 , ZrO_2 , and Fe_2O_3 were used as supports. As discussed in the previous paper,⁷ the reason for the high activity of Pd/ CeO_2 and Pd/ TiO_2 can be assigned to the promotion of reduction–oxidation cycles of supported Pd particles and the oxygen supply from the supports. It should be noted that the order of the activity was not dependent on the surface area or Pd dispersion. Although Pd dispersion of Pd/ CeO_2 is less than a half of that of Pd/ Al_2O_3 , T_{20} of the former was 71 °C lower than that of the latter. The lowest T_{20} (44 °C) was obtained when homemade $\text{TiO}_2(\text{A})$ was used as a support. Interestingly, Pd/ $\text{TiO}_2(\text{B})$ available in a market did not show such high activity at lower temperatures. The higher Pd dispersion on Pd/ $\text{TiO}_2(\text{A})$ than Pd/ $\text{TiO}_2(\text{B})$ is one of the possible reasons for the lowest T_{20} . However, T_{80} of both the Pd/ TiO_2 was almost the same. The loss of the advantage of Pd/ $\text{TiO}_2(\text{A})$ at higher temperature is not caused by sintering of Pd particles on Pd/ $\text{TiO}_2(\text{A})$ because the activity patterns of all the catalysts were reproducible. The result suggests that the promotion effect is caused by an interaction between Pd and $\text{TiO}_2(\text{A})$, which is limited below 100 °C. As shown in Fig. 1S,[†] both the TiO_2 supports showed the diffraction lines of anatase phase, while the intensity of the diffraction lines of $\text{TiO}_2(\text{A})$ were significantly weaker than those of $\text{TiO}_2(\text{B})$. The result suggests major amorphous phase in $\text{TiO}_2(\text{A})$ may cause the promotive effect of CO oxidation at lower temperatures. In order to obtain more active catalyst, a design of a support is investigated using TiO_2 and CeO_2 in the next section.

3.2. Design of TiO_2 – CeO_2 support

Fig. 1 shows the activity patterns of Pd catalysts supported on CeO_2 , $\text{TiO}_2(\text{A})$, and their mixed oxides. The activity pattern of

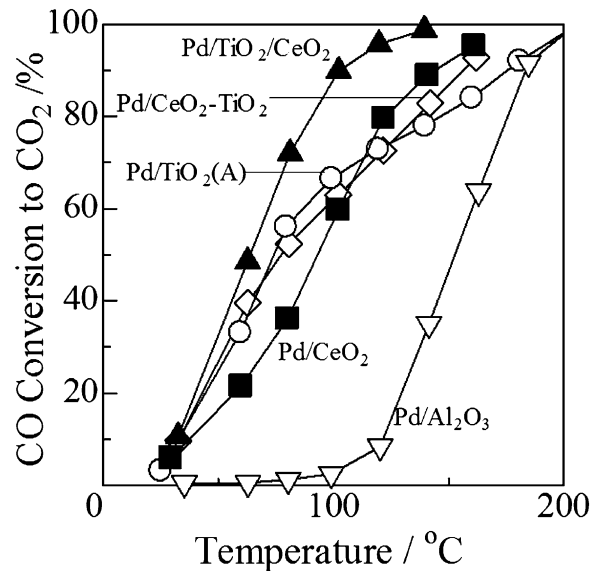


Fig. 1 Conversion of CO over 1 wt% Pd supported catalysts.

Pd/ Al_2O_3 was also plotted as a model of practical catalyst. Although the conversion of CO on Pd/ TiO_2 is higher than Pd/ CeO_2 below 110 °C, the increase in CO conversion on Pd/ $\text{TiO}_2(\text{A})$ slowed down above 100 °C and became the same as Pd/ Al_2O_3 above 180 °C. Assuming that the mixing of CeO_2 and TiO_2 may result in a better performance, two types of supports were examined, *i.e.*, CeO_2 – TiO_2 mixed oxide^{38–44} and TiO_2 – CeO_2 supported oxide. The CO oxidation activity of Pd/ CeO_2 – TiO_2 ($\text{Ce}/\text{Ti} = 0.2$) was comparable to Pd/ TiO_2 below 80 °C, however, that was lower than Pd/ CeO_2 above 110 °C. On the other hand, after the optimization of chemical composition and preparation conditions, Pd/ TiO_2 – CeO_2 ($\text{TiO}_2 = 5.4$ wt%) showed the best activity from the light-off to the 100% conversion. The surface area and Pd dispersion of Pd/ TiO_2 – CeO_2 were $64 \text{ m}^2 \text{ g}^{-1}$ and 35%, respectively. Since the Pd dispersions of Pd/ TiO_2 – CeO_2 and Pd/ CeO_2 – TiO_2 are the same, the better activity of Pd/ TiO_2 – CeO_2 than Pd/ CeO_2 – TiO_2 is caused by another factor, as discussed in the Section 3.3. Interestingly, the CO conversion over Pd/ TiO_2 – CeO_2 – ZrO_2 ($\text{TiO}_2 = 5.4$ wt%, $\text{Ce}/\text{Zr} = 5/5$) did not exceed that of Pd/ CeO_2 (figure not shown). It should be noted that Pd/ TiO_2 – CeO_2 showed the CO oxidation activity around 100 °C lower than Pd/ Al_2O_3 which is a typical oxidation catalyst. The optimization of the chemical compositions and preparation conditions is reported below.

Fig. 2 shows the effect of TiO_2 content on the CO oxidation activity of Pd/ TiO_2 – CeO_2 . The catalytic activity increased with the increase in the TiO_2 content up to 5.4 wt%, and further addition of TiO_2 suppressed the catalytic activity. It is interesting that the maximum activity was obtained when the theoretical amount of monolayer TiO_2 (5.4 wt%) was supported on CeO_2 .

Fig. 3 shows the effect of TiO_2 precursors and precipitation temperature on the CO oxidation activity of Pd/ TiO_2 – CeO_2 . Using TiCl_4 as a precursor, the precipitation at 4 °C (water/ice bath) resulted in the better catalytic performance than that

Table 1 BET surface area (S_{BET}), dispersion of Pd (D_{Pd}), and temperatures at which CO conversions were 20% and 80% (T_{20} and T_{80}) for 1 wt% Pd supported catalysts

Catalysts	$S_{\text{BET}}/\text{m}^2 \text{ g}^{-1}$	$D_{\text{Pd}}/\%$	$T_{20}/^\circ\text{C}$	$T_{80}/^\circ\text{C}$
Pd/ $\text{TiO}_2(\text{A})$	56	69	44	147
Pd/ CeO_2	84	32	59	122
Pd/ CeO_2 – ZrO_2	36	12	71	168
Pd/ $\text{TiO}_2(\text{B})$	130	23	84	151
Pd/ CeO_2 – TiO_2	200	35	88	138
Pd/ Al_2O_3	242	71	130	176
Pd/ SiO_2	414	16	149	<200
Pd/ ZrO_2	11	10	155	195
Pd/ Fe_2O_3	7.0	0.1	183	200

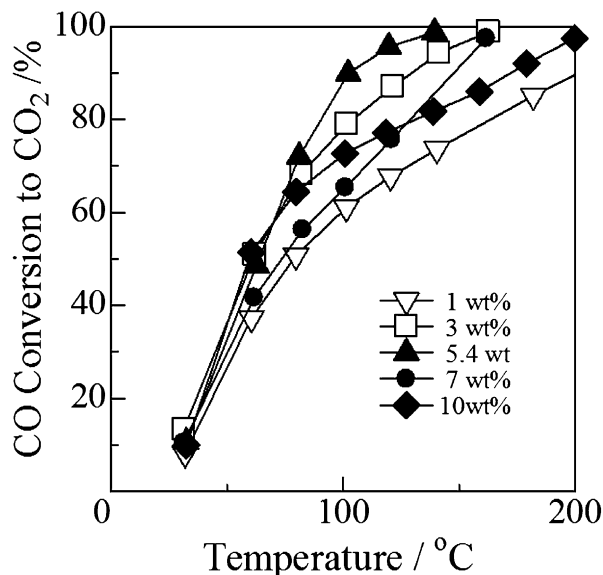


Fig. 2 Conversion of CO over Pd/TiO₂-CeO₂ having various TiO₂ contents.

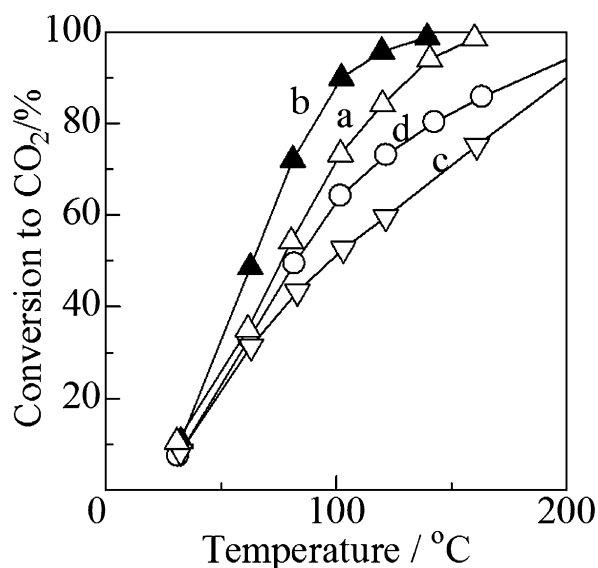


Fig. 3 Conversion of CO over Pd/TiO₂-CeO₂ catalysts. The TiO₂-CeO₂ supports were prepared using (a-c) TiCl₄, and (d) Ti(OC₃H₇)₄ as precursors and precipitated at (a) room temperature, (b) 4 °C, (c) -20 °C, and (d) 4 °C.

precipitated at room temperature. The further decrease in the temperature to -20 °C (NaCl/water/ice bath) was not effective. The use of Ti(OC₃H₇)₄ as a precursor was less effective than that of TiCl₄. The best catalyst performance was obtained when 5.4 wt% TiO₂ was precipitated to CeO₂ at 4 °C using TiCl₄ as a precursor. The EDX images of the optimized support indicated uniform dispersion of TiO₂ on CeO₂ support, as shown in Fig. 2S.† In the XRD pattern, there was no diffraction line assignable to TiO₂, indicating TiO₂ is in amorphous phase, very small particle, or thin layer. The promotion effect of TiO₂ layer

on the CO oxidation suggests contacts between TiO₂ and Pd particles. The promotive role of surface TiO₂ is investigated in the next section.

3.3. Promotion effect of surface TiO₂ on CeO₂

As discussed in the previous paper, the catalytic activity of supported Pd catalysts for the low temperature oxidation of CO can be rationalized by the following factors: (1) reducibility of supported Pd species, (2) oxygen storage-release property of the supports, and (3) dispersion of Pd.⁷ The factor (1) is essential for the activation of CO because coordinatively unsaturated surface sites of Pd metal particles are necessary for CO adsorption. The factor (2) is essential for the activation of O₂. Since the Pd dispersions of Pd/TiO₂-CeO₂, Pd/CeO₂, and Pd/CeO₂-TiO₂ were almost the same and lower than Pd/TiO₂, the factor (3) can be neglected as the reason for the best activity of Pd/TiO₂-CeO₂. Therefore, the factors (1) and (2) of Pd/TiO₂-CeO₂ are compared with Pd/CeO₂ and Pd/TiO₂.

The oxygen storage-release property was evaluated by weight deviation during the O₂-H₂ periodic operation at 300 °C, and the results of Pd/TiO₂, Pd/CeO₂, and Pd/TiO₂-CeO₂ are shown in Fig. 4. It is clear that the maximum weight decrease is strongly dependent on the supports in the following order: Pd/TiO₂-CeO₂ (0.19 mmol-O₂ g⁻¹) ≥ Pd/CeO₂ (0.14 mmol-O₂ g⁻¹) ≫ Pd/TiO₂ (0.07 mmol-O₂ g⁻¹). The weight deviation of Pd/CeO₂ corresponds to the reduction of pure CeO₂ to CeO_{2-δ} (δ = 0.048), which is close to the maximum oxygen storage capacity for pure CeO₂ (δ = 0.05).^{27,29} On the other hand, the released oxygen from Pd/TiO₂ was only a half of that from Pd/CeO₂. The oxygen storage capacity of CeO₂ was retained after TiO₂ modification. The trend was the same at 200 °C: the maximum weight decreases were Pd/TiO₂-CeO₂ (0.17 mmol-O₂ g⁻¹) ≥ Pd/CeO₂ (0.14 mmol-O₂ g⁻¹) ≫ Pd/TiO₂ (undetectable). The rates for oxygen release and storage at 300 °C was estimated from the initial slope of the weight deviation, as shown in Fig. 3S.† The estimated release rates were 0.54 × 10⁻⁶ mol-O₂ g⁻¹ s⁻¹ for Pd/

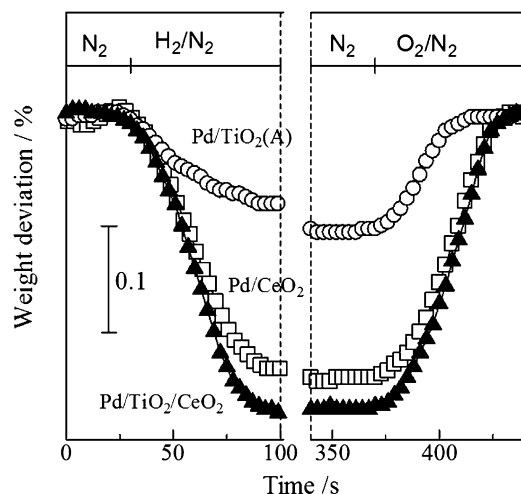


Fig. 4 Weight deviation of Pd/TiO₂, Pd/CeO₂, and Pd/TiO₂-CeO₂ during O₂-H₂ periodic operation at 300 °C.

TiO₂(A), and 1.8×10^{-6} mol-O₂ g⁻¹ s⁻¹ for Pd/CeO₂ and Pd/TiO₂-CeO₂. Pd/CeO₂ and Pd/TiO₂-CeO₂ showed 3.3 times faster rate than Pd/TiO₂(A). The oxygen storage rates of these three catalysts are the same (0.94×10^{-6} mol-O₂ g⁻¹ s⁻¹). The results suggest the oxygen storage-release capacity and rate at 300 °C of Pd/TiO₂-CeO₂ were comparable to Pd/CeO₂, indicating the contribution of OSC on higher CO conversion level. The lower activity of Pd/TiO₂(A) at higher temperatures can be rationalized by the lower oxygen storage capacity and release rate. Actually, above 180 °C, Pd/TiO₂(A) showed comparable activity to Pd/Al₂O₃ having no oxygen storage capacity.

As discussed above, the contribution of OSC on CO oxidation above 100 °C can be rationalized, but the contribution of OSC on the light-off activity cannot be discussed based on TG-DTA results because the weight deviation during the H₂-O₂ periodic operation was negligible below 100 °C. Mukri and co-workers reported that Ti_{1-x}Pd_xO_{2-x} prepared by substitution of TiO₂ by Pd²⁺ ion showed high catalytic activity for CO oxidation because of activated lattice oxygen.²¹ In their case, the formation Pd-O-Ti interface in lattice improved the catalytic activity due to high oxygen storage capacity up to 5.1 mmol g⁻¹, which was more than one order of magnitude higher than those for the catalysts in this study. Thus, the promotion effect of the TiO₂ layer cannot be attributed only to OSC enhancement. The different type of the effect of TiO₂ layer on Pd species can be expected. Therefore, reduction-oxidation property of the catalysts below 100 °C was evaluated by CO-Temperature Programmed Reduction and *in situ* XANES.

Fig. 5 shows CO-Temperature Programmed Reduction (CO-TPR) profiles of selected Pd supported catalysts. Before the TPR measurement, the supported Pd was oxidized to PdO, and the TPR measurement was carried out in 0.4% CO/N₂ without O₂. Pd/Al₂O₃ showed a reduction peak around 165 °C. The amount of evolved CO₂ (0.11 mmol g⁻¹) in the first peak was almost equivalent to the stoichiometry of PdO reduction to Pd (0.094 mmol g⁻¹). The other catalysts showed two reduction peaks below 150 °C and above 150 °C. As for the first peak, the amount of evolved CO₂ (0.13 mmol g⁻¹ for Pd/TiO₂, 0.37 mmol g⁻¹ for Pd/CeO₂, and 0.40 mmol g⁻¹ for Pd/TiO₂-CeO₂,

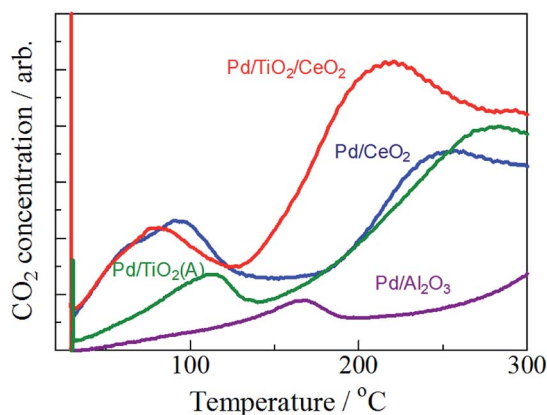


Fig. 5 Effluent CO₂ profile during CO-Temperature Programmed Reduction of supported Pd catalysts.

respectively) was higher than the stoichiometry of the PdO reduction to metallic Pd. The excess formation of CO₂ is caused by the oxygen release from the supports.⁷ The reduction peak above 150 °C is attributed to the contribution of supports or disproportionation of CO. The maximum reduction temperature of the first peak was in the order of Pd/TiO₂-CeO₂ (78 °C) < Pd/CeO₂ (96 °C) < Pd/TiO₂ (113 °C) ≪ Pd/Al₂O₃ (165 °C). This order was not well in harmony with that of CO oxidation activity, because the reduction temperature of Pd/TiO₂ was higher than Pd/CeO₂ and the positions of the first peak of Pd/TiO₂-CeO₂ and Pd/CeO₂ are too close on both temperature and quantity to attribute the big difference in the CO conversion at 60 °C for these catalysts (21% for Pd/CeO₂ and 48% for Pd/TiO₂-CeO₂, respectively). From the results of CO-TPR, we cannot conclude that the catalytic activity is controlled by the reducibility of supported Pd species from PdO_x to Pd or OSC. Then, to investigate the oxidation step of supported Pd particles (from Pd to PdO_x), *in situ* XANES spectra are compared.

Fig. 6 shows *in situ* Pd K-edge XANES spectra of supported Pd catalysts under the CO oxidation conditions below 100 °C. The feed gas compositions are the same as in the catalytic tests. Under the CO oxidation, the spectra of supported Pd catalysts are similar to that after the reduction in H₂, indicating the supported Pd species is basically in metallic state. However, the shift of the absorption edge to the higher energy suggests certain contribution of oxidized Pd species. The oxidation state of Pd was evaluated in the following manner. Because of the interaction between Pd species and supports, the spectra were not reproduced by the combination of the spectra of pure PdO disk and Pd foil. Therefore, we used the spectra of catalysts after calcination as a reference of oxidized state (Ox. in the figures)

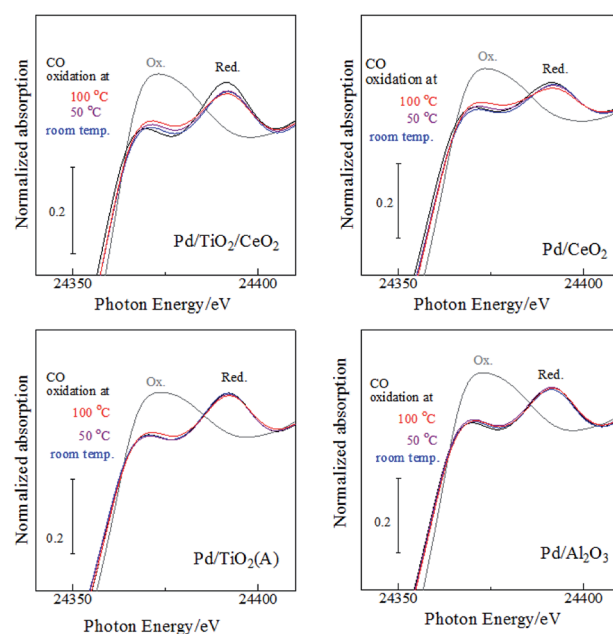
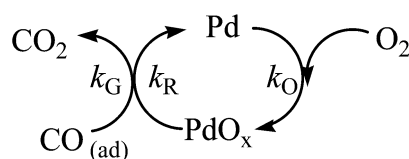


Fig. 6 Pd K-edge XANES spectra of supported Pd catalysts (Ox.) after calcination at 500 °C in air, (Red.) after reduction in H₂ at 400 °C for 30 min, and *in situ* Pd K-edge XANES spectra under the CO oxidation at various temperatures.

and after reduction in H₂ at 400 °C as a reference of reduced state (Red. in the figures). The measured *in situ* XANES spectra were well reproduced by the combination of these reference spectra. Table 2 shows the evaluated contribution of oxidized Pd under the CO oxidation. The oxidation state of Pd was strongly affected by the supports. The contribution of oxidized Pd was less than 10% on Pd/Al₂O₃ which was not active for the CO oxidation below 100 °C. On the other hand, more than 10% of Pd is oxidized on TiO₂-CeO₂ and TiO₂ supports even at room temperature. With the increase in the reaction temperature, the oxidation number of Pd increased for all the catalysts. Although the contribution of oxidized Pd in Pd/CeO₂ was lower than that of Pd/TiO₂-CeO₂ below 50 °C, they were almost the same at 100 °C. As for Pd/TiO₂, the contribution of oxidized Pd was comparable to that of Pd/TiO₂-CeO₂ at room temperature, while that was not sensitive to reaction temperature. The trend in the oxidation state of Pd is in harmony with the CO oxidation activity. The results in the table suggest contribution of the oxidation step of Pd under the CO oxidation as an activity-controlling factor.

One may wonder above discussion: although the reducibility of Pd is one of the activity-controlling factors, the promotion effect of TiO₂ modification was attributed to the rate of oxidation of Pd. The results can be rationalized by considering the reduction-oxidation cycle of Pd species during the CO oxidation. The oxidation of CO over Pd catalyst can be generally depicted in the following scheme.



In lean conditions (oxygen-rich atmospheres), Pd species are partially oxidized by gaseous oxygen or oxygen from supports. The oxidation of CO proceeds with the reduction of PdO_x to metallic Pd. The rates for both Pd oxidation (k_O) and PdO_x reduction (k_R) determine the activity of gas phase CO oxidation (k_G). Comparing Pd/TiO₂-CeO₂ and Pd/CeO₂, the rates of PdO_x reduction to Pd (k_R) by CO are not much different because the reduction peaks in CO-TPR were observed at the same temperature range. It suggests that the rate determining step is the regeneration of PdO_x species (k_O). Although the rate of PdO_x regeneration cannot be evaluated, the oxidation state under the reaction conditions estimated by XANES spectra indicates the

equilibrium constant ($K = k_O/k_R$) under the reaction conditions. The contribution of PdO_x under the reaction conditions should indicate the relative difference of K in each sample, and Pd species on Pd/TiO₂-CeO₂ is more easily oxidized than that on Pd/CeO₂ at lower temperatures. The results indicate that the promotive effect of TiO₂ can be attributed to the promotion of the regeneration step of oxidized PdO_x species. The promotive effect was limited at lower temperatures, *i.e.*, contributions of oxidized Pd were much higher on Pd/TiO₂-CeO₂ and Pd/TiO₂, while at 100 °C that of Pd/CeO₂ became almost the same as Pd/TiO₂-CeO₂ but Pd/TiO₂ showed lower value. The variation in the PdO_x ratio as a function of reaction temperature is approximately in harmony with the activity pattern for CO oxidation shown in Fig. 1. Therefore, it is reasonable to attribute the promotive effect of TiO₂ modification to the promotion of re-oxidation step of Pd species under the CO oxidation.

4. Conclusions

The effect of metal oxide support was investigated to promote the CO oxidation over supported Pd catalysts at lower temperatures. The use of TiO₂ support enhanced the CO oxidation below 100 °C, and that of CeO₂ support was effective above 100 °C. Applying the advantages of CeO₂ and TiO₂, Pd/TiO₂-CeO₂ showed the best catalytic activity from the light-off to the 100% conversion, which was around 100 °C lower than Pd/Al₂O₃. After the optimization of the chemical compositions and preparation conditions, the best catalyst performance was obtained when theoretical monolayer amount (5.4 wt%) of TiO₂ was precipitated to CeO₂ at 4 °C using TiCl₄ as a precursor. By using TG-DTA, CO-TPR, and *in situ* XANES, the promotion of the oxidation step of Pd species during the CO oxidation was revealed to be an activity-controlling factor.

Acknowledgements

This work was partly supported by JSPS KAKENHI Grant from the Ministry of Education, Culture, Sports, Science and Technology, Japan. A part of this work was performed under a management of "Elements Strategy Initiative for Catalysts & Batteries (ESICB)" supported by MEXT program "Elements Strategy Initiative to Form Core Research Centre" (since 2012), MEXT; Ministry of Education Culture, Sports, Science and Technology, Japan. The XAFS measurements at SPring-8 were carried out by the approval (proposal no. 2012B1569) of the Japan Synchrotron Radiation Research Institute (JASRI).

Notes and references

- 1 A. Baylet, S. Royer, P. Marecot, J. M. Tatibouet and D. Duprez, *Appl. Catal., B*, 2008, **77**, 237–247.
- 2 Y. Nishihata, J. Mizuki, T. Akao, H. Tanaka, M. Uenishi, M. Kimura, T. Okamoto and N. Hamada, *Nature*, 2002, **418**, 164–167.
- 3 Y. Nagai, T. Hirabayashi, K. Dohmae, N. Takagi, T. Minami, H. Shinjoh and S. Matsumoto, *J. Catal.*, 2006, **242**, 103–109.

Table 2 Contribution of oxidized Pd in Pd particles (% in total Pd) under the CO oxidation at various temperatures evaluated from *in situ* XANES spectra

Catalyst	Room temp.	50 °C	100 °C
Pd/TiO ₂ -CeO ₂	16.2	18.9	23.6
Pd/CeO ₂	7.4	13.7	23.7
Pd/TiO ₂ (A)	10.7	13.1	16.9
Pd/Al ₂ O ₃	4.0	4.7	6.8

- 4 R. V. Gulyaev, A. I. Stadnichenko, E. M. Slavinskaya, A. S. Ivanova, S. V. Koscheev and A. I. Boronin, *Appl. Catal., A*, 2012, **439–440**, 41–50.
- 5 A. Satsuma, R. Sato, K. Osaki and K. Shimizu, *Catal. Today*, 2012, **185**, 61–65.
- 6 K. B. Kim, M. K. Kim, Y. H. Kim, K. S. Song and E. D. Park, *Res. Chem. Intermed.*, 2010, **36**, 603–611.
- 7 A. Satsuma, K. Osaki, M. Yanagihara, J. Ohya and K. Shimizu, *Appl. Catal., B*, 2013, **132–133**, 511–518.
- 8 R. F. Hicks, H. Qi, M. L. Young and R. G. Lee, *J. Catal.*, 1990, **122**, 295–306.
- 9 R. Burch, P. K. Loader and F. J. Urbano, *Catal. Today*, 1996, **27**, 243–248.
- 10 H. Yoshida, T. Nakajima, Y. Yazawa and T. Hattori, *Appl. Catal., B*, 2007, **71**, 70–79.
- 11 P. Castellazzi, G. Groppi, P. Forzatti, E. Finocchio and G. Busca, *J. Catal.*, 2010, **275**, 218–227.
- 12 S. Colussi, A. Trovarelli, E. Vesselli, A. Baraldi, G. Comelli, G. Groppi and J. Llorca, *Appl. Catal., A*, 2010, **390**, 1–10.
- 13 T. Schalow, B. Brandt, M. Laurin, S. Schauerermann, S. Guimond, H. Kuhlbeck, J. Libuda and H.-J. Freund, *Surf. Sci.*, 2006, **600**, 2528–2542.
- 14 S. Specchia, E. Finocchio, G. Busca, P. Palmisano and V. Specchia, *J. Catal.*, 2009, **263**, 134–145.
- 15 S. Specchia, E. Finocchio, G. Busca, G. Saracco and V. Specchia, *Catal. Today*, 2009, **143**, 86–93.
- 16 M. S. Hedge, G. Madras and K. C. Patil, *Acc. Chem. Res.*, 2009, **42**, 704–712.
- 17 P. Bera, A. Gayen, M. S. Hedge, N. P. Lalla, L. Spadaro, F. Fursteri and F. Arena, *J. Phys. Chem. B*, 2003, **107**, 6122–6130.
- 18 T. Baidya, A. Gayen, M. S. Hegde, N. Ravishankar and L. Dupont, *J. Phys. Chem. B*, 2006, **110**, 5262–5267.
- 19 T. Baidya, M. S. Hegde, N. Ravishankar, A. Marimuthu and G. Madras, *J. Phys. Chem. C*, 2007, **111**, 830–839.
- 20 T. Baidya, G. Dutta, M. S. Hegde and U. V. Waghmare, *Dalton Trans.*, 2009, 455–464.
- 21 B. D. Mukri, G. Dutta, U. V. Waghmare and M. S. Hegde, *Chem. Mater.*, 2012, **24**, 4491–4502.
- 22 M. Kurnatowska, L. Kepinski and W. Mista, *Appl. Catal., B*, 2012, **117–118**, 135–147.
- 23 S. Colussi, A. Gayen, M. F. Camellone, M. Boaro, J. Llorca, S. Fabis and A. Trovarelli, *Angew. Chem., Int. Ed.*, 2009, **48**, 8481–8484.
- 24 L. Liu, F. Zhou, L. Wang, X. Qi, F. Shi and Y. Deng, *J. Catal.*, 2010, **274**, 1–10.
- 25 K. Ikeue, K. Watanabe, T. Minekishi, A. Imamura, T. Sato, Y. Nagao, Y. Nakahara and M. Machida, *Appl. Catal., B*, 2014, **146**, 50–56.
- 26 H. C. Yao and F. Y. Yao, *J. Catal.*, 1984, **86**, 254–265.
- 27 M. Ozawa, M. Kimura and A. Isogai, *J. Alloys Compd.*, 1993, **193**, 73–75.
- 28 M. Sugiura, M. Ozawa, A. Suda, T. Suzuki and T. Kanazawa, *Bull. Chem. Soc. Jpn.*, 2005, **78**, 752–767.
- 29 G. Dutta, U. Vaghmare, T. Baidya, M. S. Hegde, K. R. Priolkar and P. R. Sarode, *Catal. Lett.*, 2006, **108**, 165–172.
- 30 G. Dutta, U. Vaghmare, T. Baidya, M. S. Hegde, K. R. Priolkar and P. R. Sarode, *Chem. Mater.*, 2006, **18**, 3249–3256.
- 31 Q. Ding, S. Yin, C. Guo and T. Sato, *Chem. Lett.*, 2012, **41**, 1250–1252.
- 32 T. Jin, T. Okuhara, G. J. Mains and J. M. White, *J. Phys. Chem.*, 1987, **91**, 3310–3315.
- 33 G. S. Zafiris and R. J. Gorte, *J. Catal.*, 1993, **139**, 561–567.
- 34 H. Cordatos and R. J. Gorte, *J. Catal.*, 1996, **159**, 112–118.
- 35 J.-Y. Luo, M. Meng, X. Li, X.-G. Li, Y.-Q. Zha, T.-D. Hu, Y.-N. Xie and J. Zhang, *J. Catal.*, 2008, **254**, 310–324.
- 36 A. Tömcróna, M. Skoglundh, P. Thormählen, E. Fridell and E. Jobson, *Appl. Catal., B*, 1997, **14**, 131–146.
- 37 A. Martínez-Arias, M. Fernández-García, A. Iglesias-Juez, A. B. Hungria, J. A. Anderson, J. C. Conesa and J. Soria, *Appl. Catal., B*, 2001, **31**, 39–50.
- 38 G. Dong, J. Wang, Y. Gao and S. Chen, *Catal. Lett.*, 1999, **58**, 37–41.
- 39 H. Zhu, Z. Qin, W. Shan, W. Shen and J. Wang, *J. Catal.*, 2004, **225**, 267–277.
- 40 H. Zhu, Z. Qin, W. Shan, W. Shen and J. Wang, *J. Catal.*, 2005, **233**, 41–50.
- 41 H. Zhu, Z. Qin, W. Shan, W. Shen and J. Wang, *Catal. Today*, 2007, **126**, 382–386.
- 42 S. Yang, W. Zhu, Z. Jiang, Z. Chen and J. Wang, *Appl. Surf. Sci.*, 2006, **252**, 8499–8505.
- 43 F. Liang, H. Zhu, Z. Qin, G. Wang and J. Wang, *Catal. Commun.*, 2009, **10**, 737–740.
- 44 K. Nakagawa, Y. Murata, M. Kishida, M. Adachim, M. Hiro and K. Susa, *Mater. Chem. Phys.*, 2007, **104**, 30–39.
- 45 H. Zou and Y. S. Lin, *Appl. Catal., A*, 2004, **265**, 35–42.
- 46 T. Tanabe, Y. Nagai, T. Hirabayashi, N. Takagi, K. Dohmae, N. Takahashi, S. Matsumoto, H. Shinjoh, J. N. Kondo, J. C. Schouten and H. H. Brongersma, *Appl. Catal., A*, 2009, **370**, 108–113.
- 47 K. Shimizu, Y. Saito, T. Nobukawa, N. Miyoshi and A. Satsuma, *Catal. Today*, 2008, **139**, 24–28.
- 48 K. Shimizu, Y. Saito, T. Nobukawa and A. Satsuma, *Top. Catal.*, 2010, **53**, 584–590.